Synchronous whirling of spinning homogeneous elastic cylinders: linear and weakly nonlinear analyses

Serge Mora

Synchronous whirling of spinning homogeneous elastic cylinders: linear and weakly non-linear analyses

Serge Mora[1]

[1] *Laboratoire de Mécanique et Génie Civil, Université de Montpellier and CNRS, France**

(Dated: April 5, 2020)

Stationary whirling of slender and homogeneous (continuous) elastic shafts rotating around their axis, with pin-pin boundary condition at the ends, is revisited by considering the complete deformations in the cross section of the shaft. The stability against a synchronous sinusoidal disturbance of any wave length is investigated and the analytic expression of the buckling amplitude is derived in the weakly non-linear regime by considering both geometric and material (hyper-elastic) non-linearities. The bifurcation is super-critical in the long wave length domain for any elastic constitutive law, and sub-critical in the short wave length limit for a limited range of non-linear material parameters.

PACS numbers: 46.32.+x,46.25.-y,83.10.Gr, 05.45.-a

I. INTRODUCTION

A homogeneous and balanced elastic cylinder rotating around its axis is unstable beyond a critical angular velocity, leading to transverse deformations and whirling if the ends of the cylinder are constraint for instance with bearings. This instability results from the competition between the destabilizing effect of the centrifugal force that tends to drive the cylinder away from the axis of rotation, and the elastic forces opposed to the deformation.

The whirling of rotating cylinders, as well as the propagation of vibrations in the neighborhood of the critical angular velocity, have been extensively investigated in the context of rotor-dynamics [1, 2] because of their damaging effects on the smooth running of rotating machinery such as compressors, pumps, turbines, turbochargers, jet engines [3]. Understanding the stability of spinning shafts and their post-buckling behavior is crucial for the success in the design of this kind of rotating systems.

While most of the studies have dealt with small deformations linearized at leading order [4], few studies have considered non-linear effects [5, 6]. The non-linear dynamic behaviour of a uniform, slender rotating shaft made of a viscoelastic material with external damping mechanism has been studied by considering geometric non-linearities resulting from large transverse displacements [7–9]. Using the center manifold technique [10] and the normal form method, the effects of external and internal damping on the whirling of rotating shafts have been investigated in terms of Hopf or double eigenvalues bifurcations. By pushing expansions up to order 2 in terms of the characteristic magnitude of the infinitesimal strain, ε, but Hookean elasticity for the strain-stress relation, the whirling amplitude in steady state configurations have been computed as the radius of a limit cycle in phase portraits [9]. However, the intrinsic non-linear features of material constitutive law have been neglected in these studies. Indeed, order ε^2 in the expansion of the governing equations originates both from geometrical non-linearities (arising from the expression of the local curvature of the center line of the cylinder) together with non-linearities in the constitutive law of the elastic material. These last non-linearities are essential in order to fulfilled the requirement of material objectivity [11].

An expansion of the bending energy based on a scalar non-linear constitutive law [12] has been proposed in order to calculate non-synchronous whirling of rotating shafts [13]. Because of the scalar features of the constitutive law used by the author, this approach is limited to deformation with large wave length (compared with the radius of the shaft) and the issues related to Poisson effect are ignored. In addition, the rotating shaft was supposed to be not extensible which is not relevant for pin-pin ends since the extension of the center-line with pin-pin ends is of order ε^2 and cannot be neglected.

A linear analysis of the whirling bifurcation of infinite rotating cylinders under axial tension has been developed in [14], based on non-linear constitutive equations in three dimensions so that this analysis is relevant for any wave length of the deformation, but the non-linear analysis is still missing. In previous papers [15, 16], the bifurcations of spinning undeformable shafts, surrounded by a compliant elastic layer, have been investigated both in the linear and the non-linear regimes, under plane strain assumption.

*Corresponding author: serge.mora@umontpellier.fr

In this paper, a non-linear analysis of the *stationary* whirling of *homogeneous* rotating cylinders is developed, based on the hypothesis of negligible external damping [4] so that the system is conservative. The steady states are reached once transient vibrations are damped thanks to dissipative processes (internal damping) occurring inside the elastic material. The cylinders are supposed to be slender, their length L being far larger than the radius r_0. The elastic material is assumed to be isotropic and incompressible. The buckling amplitude of synchronous and steady sinusoidal perturbations of any wave length is calculated without any further assumption for the constitutive law of the elastic material. The analysis relies on the complete three dimensional equations so that the results are relevant for any wave length of the whirling, including wave length of the same order of magnitude as the radius of the shaft. The complete (non-linear) equations governing the equilibrium steady states are derived in Section II. A Lagrange multiplier accounts for the incompressibility constraint and the equations for the three components of displacement field are established in strong form. Section III is devoted to the linear stability analysis. The critical angular velocity is found to depend on the shear modulus of the elastic material, its mass density, the radius of the rotating cylinder, and in a non trivial manner on the ratio of the wave length of the deformation to the radius of the cylinder. The weakly non-linear analysis of the bifurcation is carried out in Section IV. The bifurcation is found to be super-critical for neo-Hookean materials, and can be sub-critical at small wave length for particular constitutive laws. Predictions of sections III-IV are checked in Section V by means of numerical simulations based on the Finite Element Method. The last part (Section VI) of the paper is devoted to a conclusion.

II. EQUILIBRIUM EQUATIONS BASED ON A FINITE STRAIN THEORY

In this section the non-linear equations governing the equilibrium (steady) configurations of a rotating elastic cylinder are derived, considering an arbitrary hyper-elastic incompressible isotropic material.

Let r_0 denote the radius of the undeformed cylinder, ρ its mass density and μ its initial shear modulus, *i.e.* the shear modulus for infinitesimal strain. The cylinder is spun with an angular velocity ω about its axis, as sketched in Figure 1. In the co-rotating frame, both the elastic force and the centrifugal force are conservative. The equilibrium

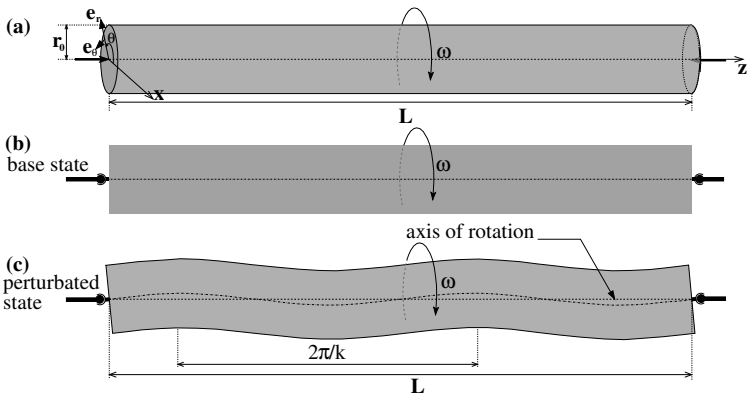

FIG. 1: Sketches of an elastic cylinder of length L and radius r_0 rotating around its axis with the angular velocity ω. The two ends of the cylinder are pinned at the axis. (a) Three dimensional view of the reference (unbuckled) configuration. (b) Side view of this reference configuration. (c) Side view of a perturbation of characteristic wave vector k parallel to the axis.

can therefore be derived from the condition that the total potential energy is stationary. The position $\mathbf{R}$ of a material point in the deformed configuration is given as a map $\mathbf{R}(\mathbf{r})$ in terms of the position $\mathbf{r}$ in the undeformed configuration. For an isotropic and incompressible elastic material, the strain energy density is a function of the two first invariants, I_1 and I_2, of Green's deformation tensor $\mathbf{C} = \mathbf{F}^T \cdot \mathbf{F}$, where $\mathbf{F} = \partial\mathbf{R}/\partial\mathbf{r}$ is the deformation gradient:

$$\begin{aligned} I_1 &= \text{tr } \mathbf{C} - 3, \\ I_2 &= \tfrac{1}{2}\left((\text{tr } \mathbf{C})^2 - \text{tr } \left(\mathbf{C}^2\right)\right) - 3. \end{aligned} \tag{1}$$

The strain energy density is then written as $\mu W(I_1, I_2)$ where W is the dimensionless strain energy density. For the strain energy $\mu W(I_1, I_2)$ to be consistent with the initial shear modulus μ, the following normalization condition must be enforced:

$$\frac{\partial W}{\partial I_1}(0,0) + \frac{\partial W}{\partial I_2}(0,0) = \frac{1}{2}. \tag{2}$$

For an incompressible neo-Hookean solid [11, 17] and for an incompressible Mooney-Rivlin solid [18, 19], the dimensionless strain energy density are respectively $W = \frac{1}{2}(I_1 - 3)$ and $W = \frac{1}{2}\left(\beta(I_1 - 3) + (1-\beta)(I_2 - 3)\right)$, with β a material constant in the range $[0; 1]$.

Incompressibility of the elastic material imposes the condition $\mathcal{D}(\mathbf{r}) = 1$, where $\mathcal{D} = \det \mathbf{F}$ is the Jacobian of the transformation. To characterize equilibrium configurations, we seek stationary points of the augmented energy

$$\mathcal{E} = \int_{0<r<r_0;\ 0<z<L} \mathrm{d}\mathbf{r} \left(\mu\, W(I_1, I_2) - \frac{1}{2}\rho\,\omega^2 \left(\mathbf{R}\cdot\mathbf{R} - (\mathbf{R}\cdot\mathbf{e}_z)^2\right) + \mu\, q\,(\mathcal{D} - 1) \right). \tag{3}$$

The terms in the integrand are the strain energy density, the potential of the centrifugal force, and the Lagrange term taking care of the incompressibility constraint $\mathcal{D} = 1$ by means of a Lagrange multiplier $q(\mathbf{r})$. From Eq. 3, the equilibrium of the system is governed by the two dimensionless parameters in the problem, namely $\alpha = \rho\, r_0^2\, \omega^2/\mu$ and the ratio L/r_0. We use cylindrical coordinates, with r the distance to the axis, θ the angle and z the height in the unperturbed state (Figure 1). Let $\mathbf{e_r}$, $\mathbf{e}_\theta$,$\mathbf{e_z}$ be the orthonormal basis vectors associated with coordinates r, θ and z respectively. In the deformed configuration, the position $\mathbf{R}$ of a material point is $\mathbf{R} = \mathbf{r} + u(r,\theta,z)\mathbf{e_r} + v(r,\theta,z)\mathbf{e}_\theta + w(r,\theta,z)\mathbf{e_z}$. The equilibrium equations are derived from the condition that the first variation of Eq. 3 with respect to the unknowns $u(r,\theta,z)$, $v(r,\theta,z)$, $w(r,\theta,z)$ and $q(r,\theta,z)$ is zero. Let $\mathbf{t} = (u, v, w, q)$ denote the collection of unknowns, and $\delta\mathbf{t} = (\delta u, \delta v, \delta w, \delta q)$ a virtual displacement that is kinematically admissible (abbreviated as 'k.a.'), as imposed by the boundary conditions. The field $\mathbf{t}(r,\theta,z)$ is a solution of the problem if

$$\forall \delta\mathbf{t} \text{ k.a.}, \quad D\mathcal{E}(\alpha, \mathbf{t})\,[\delta\mathbf{t}] = 0. \tag{4}$$

$D\mathcal{E}(\alpha,\mathbf{t})\,[\delta\mathbf{t}]$ denotes the first variation of the energy evaluated in the configuration $\mathbf{t}$ with an increment $\delta\mathbf{t}$, also known as the first Gâteaux derivative of the functional $\mathcal{E}$ [20]. Note that the dependence of $\mathcal{E}$ with L/r_0 is not explicitly written in Eq. 4 because it is a fixed parameter in the system, contrary to α.

Defining

$$\mathcal{G} = r\left\{ W(I_1, I_2) + q(\mathcal{D} - 1) - \frac{1}{2}\frac{\alpha}{r_0^2}\left((r+u)^2 + v^2\right) \right\} \tag{5}$$

and integrating by parts Eq. 4, we obtain the equations in the interior of the body as

$$\mathcal{D} - 1 = 0, \tag{6}$$

$$\frac{\partial \mathcal{G}}{\partial u} - \frac{\partial}{\partial r}\left(\frac{\partial \mathcal{G}}{\partial u_{,r}}\right) - \frac{\partial}{\partial \theta}\left(\frac{\partial \mathcal{G}}{\partial u_{,\theta}}\right) - \frac{\partial}{\partial z}\left(\frac{\partial \mathcal{G}}{\partial u_{,z}}\right) = 0, \tag{7}$$

$$\frac{\partial \mathcal{G}}{\partial v} - \frac{\partial}{\partial r}\left(\frac{\partial \mathcal{G}}{\partial v_{,r}}\right) - \frac{\partial}{\partial \theta}\left(\frac{\partial \mathcal{G}}{\partial v_{,\theta}}\right) - \frac{\partial}{\partial z}\left(\frac{\partial \mathcal{G}}{\partial v_{,z}}\right) = 0, \tag{8}$$

$$\frac{\partial \mathcal{G}}{\partial w} - \frac{\partial}{\partial r}\left(\frac{\partial \mathcal{G}}{\partial w_{,r}}\right) - \frac{\partial}{\partial \theta}\left(\frac{\partial \mathcal{G}}{\partial w_{,\theta}}\right) - \frac{\partial}{\partial z}\left(\frac{\partial \mathcal{G}}{\partial w_{,z}}\right) = 0, \tag{9}$$

where a comma in subscript denotes a partial derivative. The first equation (Eq. 6) is the incompressibility constraint and the three other equations (Eqs. 7-9) are the equilibrium in the radial, circumferential and longitudinal directions, respectively. These equations are complemented by the condition of zero traction at the lateral boundary $r = r_0$,

$$\left.\frac{\partial \mathcal{G}}{\partial u_{,r}}\right|_{r=r_0} = \left.\frac{\partial \mathcal{G}}{\partial v_{,r}}\right|_{r=r_0} = \left.\frac{\partial \mathcal{G}}{\partial w_{,r}}\right|_{r=r_0} = 0. \tag{10}$$

In addition, the pin-pin condition at the ends imposes:

$$u(0,\theta,z) = v(0,\theta,z) = w(0,\theta,z) = 0 \text{ for } z = 0 \text{ and } z = L \tag{11}$$

and

$$\frac{\partial \mathcal{G}}{\partial u_{,z}} = \frac{\partial \mathcal{G}}{\partial v_{,z}} = \frac{\partial \mathcal{G}}{\partial w_{,z}} = 0 \text{ for } z = 0 \text{ and } z = L. \tag{12}$$

The three last boundary conditions (Eqs. 12) originate from the variation of the augmented energy at the vicinity of the ends. Since end effects are expected to spread in a domain of characteristic size r_0, their relative contribution to the total augmented energy is of order r_0/L. Hence, within the hypothesis of a slender shaft ($r_0 \gg L$), boundary

conditions Eqs. 12 are negligible. This simplification makes possible the harmonic decomposition of the deformation (with unique wave length and unique circumferential wave number, see Section III B).

The equilibrium configurations are the solutions of the system formed by Eqs. 6-11. Because of non-linearities in the equations, the analytic resolution is out of reach. In Section III A the system is resolved in the reference (undeformed) configuration. Then the magnitude of the displacement is assumed to scale as a small parameter, ε, so that it is infinitely smaller than the other length scales (r_0 and L). Eqs. 6-11 are resolved at linear order (order ε) in Section III B, and at order ε^2 in Section IV. Finally, they are solved numerically by means of finite elements in Section V.

III. LINEAR BIFURCATION ANALYSIS

A. Unbuckled solution

We start by analyzing the unbuckled configuration (base state), and label all quantities relevant to it using a subscript '0'. In this configuration, $u_0(r,\theta,z)=0$, $v_0(r,\theta,z)=0$ and $w_0(r,\theta,z)=0$. The Lagrange multiplier q is found from the radial equilibrium Eq. 7 and Eq. 10 as

$$q_0 = \frac{\alpha}{2}\left(1-(r/r_0)^2\right)+\beta-2. \tag{13}$$

Altogether, the unbuckled solution of Eqs. 6-10 is written as $\mathbf{t}_0=(u_0,v_0,w_0,q_0)$.

B. Linearization of the equations

A small perturbation is added to the unbuckled solution, and the equations of Section II are linearized with respect to the amplitude of the perturbation,

$$\mathbf{t}=\mathbf{t}_0+\varepsilon\mathbf{t}_1=\left(\varepsilon u_1(r,\theta,z),\varepsilon v_1(r,\theta,z),\varepsilon w_1(r,\theta,z),q_0(r,\theta,z)+\varepsilon q_1(r,\theta,z)\right). \tag{14}$$

We first assume a harmonic θ and z dependence of any variation of the perturbation of u, v, w and q:

$$\begin{cases} u_1 = u_1^+(r,\theta,z)=\mathcal{R}e\left(f_u(r)e^{\mathrm{i}\theta+\mathrm{i}kz}\right)\\ v_1 = v_1^+(r,\theta,z)=\mathcal{R}e\left(-\mathrm{i}f_v(r)e^{\mathrm{i}\theta+\mathrm{i}kz}\right)\\ w_1 = w_1^+(r,\theta,z)=\mathcal{R}e\left(-\mathrm{i}f_w(r)e^{\mathrm{i}\theta+\mathrm{i}kz}\right)\\ q_1 = q_1^+(r,\theta,z)=\mathcal{R}e\left(f_q(r)e^{\mathrm{i}\theta+\mathrm{i}kz}\right)\end{cases} \tag{15}$$

where k is the axial wave number. $\mathcal{R}e$ denotes the real part. The conventional complex factor $(-\mathrm{i})$ has been included for convenience, anticipating on the fact that the phase of v_1 and w_1 are shifted by $\pi/2$ compared to the phase of the two other unknowns. At linear order in ε, one obtains from Eqs. 6-9 and after the elimination of f_v, f_w and f_q, an order 6 differential equation for f_u:

$$\begin{aligned} r^5\frac{d^6f_u}{dr^6}+9r^4\frac{d^5f_u}{dr^5}f_u+\left(9r^3-3k^2r^5\right)\frac{d^4f_u}{dr^4}+\left(-18k^2r^4-12r^2\right)\frac{d^3f_u}{dr^3}+\left(3k^4r^5-9k^2r^3+9r\right)\frac{d^2f_u}{dr^2}\\ +\left(9k^4r^4+9k^2r^2-9\right)\frac{df_u}{dr}-k^6r^5f_u=0.\end{aligned} \tag{16}$$

The boundary conditions at $r=r_0$ (Eqs. 10) simplifies at order ε and can be written in term of f_u:

$$-r_0^3\frac{d^4f_u}{dr^4}f_u-6r_0^2\frac{d^3f_u}{dr^3}+\left(2k^2r_0^3-3r_0\right)\frac{d^2f_u}{dr^2}+\left(14k^2r_0^2+3\right)\frac{df_u}{dr}+\left(-k^4r_0^3-4\alpha k^2r_0\right)f_u=0 \tag{17}$$

$$\begin{aligned} -r_0^5\frac{d^6f_u}{dr^6}-9r_0^4\frac{d^5f_u}{dr^5}+\left(2k^2r_0^5-10r_0^3\right)\frac{d^4f_u}{dr^4}+\left(16k^2r_0^4+6r_0^2\right)\frac{d^3f_u}{dr^3}+\left(-k^4r_0^5+16k^2r_0^3-12r_0\right)\frac{d^2f_u}{dr^2}\\ +\left(-7k^4r_0^4-8k^2r_0^2+12\right)\frac{df_u}{dr}-5k^4r_0^3f_u=0\end{aligned} \tag{18}$$

$$\begin{aligned} r_0^5\frac{d^6f_u}{dr^6}+9r_0^4\frac{d^5f_u}{dr^5}+\left(10r_0^3-2k^2r_0^5\right)\frac{d^4f_u}{dr^4}+\left(-16k^2r_0^4-6r_0^2\right)\frac{d^3f_u}{dr^3}+\left(k^4r_0^5-24k^2r_0^3+12r_0\right)\frac{d^2f_u}{dr^2}\\ +\left(7k^4r_0^4-12\right)\frac{df_u}{dr}-3k^4r_0^3f_u=0.\end{aligned} \tag{19}$$

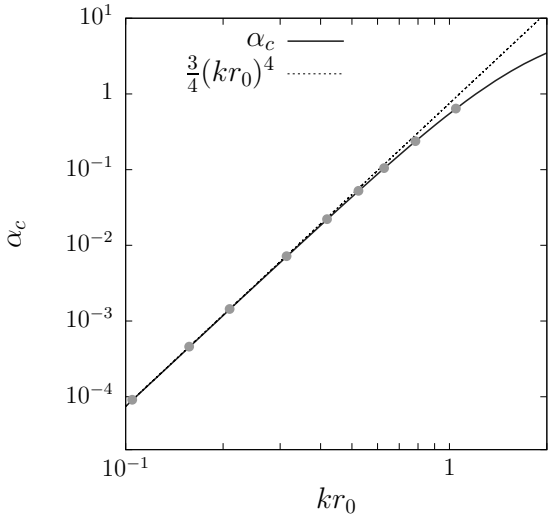

FIG. 2: Solid line: Critical value of α at the instability onset, as a function of k, calculated from Eq. 23 at order 30 in kr_0 (higher orders in the expansion lead to indistinguishable curves). Dashed line: First term in the expansion of α_c with respect to kr_0. Filled circles: Threshold α^* obtained from FEM simulations (see Eq. 46 of Section V).

C. General solution

Let $s_1(kr)$, $s_2(kr)$ and $s_3(kr)$ be three independent solutions of Eqs. 16-19 that do not diverge, as well as their first derivative, at $r = 0$. These solutions are sought as series expansions in the form:

$$s_i(kr) = \sum_{m=0}^{\infty} a_m (kr)^m. \tag{20}$$

The condition for $s_i(kr)$ to be a solution of Eq. 16 is, for $m \geq 6$:

$$a_{m-6} - 3a_{m-4}(m-4)(m-2) + 3a_{m-2}m(m-2)^2(m-4) - a_m(m-4)(m-2)^2m^2(2+m) = 0, \tag{21}$$

where a_0, a_2 and a_4 are constants that are not fixed up to now. Coefficients a_m with an odd index have to be 0. In order to build three independent solutions of Eq. 16, we choose $a_0 = 1$, $a_2 = a_4 = 0$ for $s_1(kr)$; $a_0 = a_4 = 0$ and $a_2 = 1$ for $s_2(kr)$; and $a_0 = a_2 = 0$ and $a_4 = 1$ for $s_3(kr)$. Writing now the general solution $f_u(r)$ of Eq. 16 as:

$$f_u(r) = As_1(kr) + Bs_2(kr) + Cs_3(kr), \tag{22}$$

and substituting this expression in the boundary conditions Eqs. 17-19, one gets a linear system of 3 homogeneous equations with three unknowns A, B and C. The condition for a non-zero deformation, *i.e.* $(A, B, C) \neq (0, 0, 0)$, is obtained by imposing the determinant of the linear system to be zero, leading to the condition for α, $\alpha = \alpha_c$ with α_c:

$$\alpha_c = \frac{3}{4}(kr_0)^4 - \frac{5}{24}(kr_0)^6 - \frac{19}{1536}(kr_0)^8 + \cdots \tag{23}$$

Higher orders in the expansion can be calculated as well. For $\alpha = \alpha_c$, the system is neutrally stable against a perturbation of wave number k. α_c is plotted as a function of kr_0 in Figure 2. Taking the first term in the expansion Eq. 23, one recovers the well known expression of the linear threshold calculated in the long wave length limit in the framework of Hookean elasticity, $\alpha_c = \frac{3}{4}(kr_0)^4$ (see the dashed line in Figure 2).

The expressions of functions $f_u(r)$, $f_v(r)$, $f_w(r)$ and $f_q(r)$, with the condition $f_u(r_0) = \xi$ ($\varepsilon\xi$ will be referred as the

buckling amplitude) are:

$$\frac{f_u(r)}{\xi} = 1+\left(1-\frac{r^2}{r_0^2}\right)\frac{(kr_0)^2}{4}-\left(3-\frac{4r^2}{r_0^2}+\frac{r^4}{r_0^4}\right)\frac{3(kr_0)^4}{64}+\left(23-\frac{39r^2}{r_0^2}+\frac{21r^4}{r_0^4}-\frac{5r^6}{r_0^6}\right)\frac{(kr_0)^6}{2304}+\cdots \quad (24)$$

$$\frac{f_v(r)}{\xi} = -1-\left(1+\frac{r^2}{r_0^2}\right)\frac{(kr_0)^2}{4}+\left(9+\frac{12r^2}{r_0^2}-\frac{r^4}{r_0^4}\right)\frac{(kr_0)^4}{64}-\left(23+\frac{135r^2}{r_0^2}-\frac{39r^4}{r_0^4}+\frac{r^6}{r_0^6}\right)\frac{(kr_0)^6}{2304}+\cdots \quad (25)$$

$$\frac{f_w(r)}{\xi} = \frac{r}{r_0}(kr_0)-\left(3\frac{r}{r_0}-\frac{r^3}{r_0^3}\right)\frac{(kr_0)^3}{4}+\left(\frac{7r}{r_0}-\frac{4r^3}{r_0^3}+\frac{r^5}{r_0^5}\right)\frac{(kr_0)^5}{64}+\cdots \quad (26)$$

$$f_q(r) = \frac{\xi}{r_0}\left\{\frac{r}{r_0}(kr_0)^2-\left(4\frac{r}{r_0}-\frac{r^3}{r_0^3}\right)\frac{(kr_0)^4}{8}-\left(\frac{39r}{r_0}-\frac{42r^3}{r_0^3}-\frac{r^5}{r_0^5}\right)\frac{(kr_0)^6}{192}+\cdots\right\} \quad (27)$$

Indeed, the form of Eq. 15 corresponds to a right helical deformation along the z axis. The left helical deformation can be deduced from the previous one (with the transformation $k \leftrightarrow -k$) :

$$\begin{cases} u_1 = u_1^-(r,\theta,z) = \mathcal{R}e\left(f_u(r)e^{\mathrm{i}\theta-\mathrm{i}kz}\right) \\ v_1 = v_1^-(r,\theta,z) = \mathcal{R}e\left(-\mathrm{i}f_v(r)e^{\mathrm{i}\theta-\mathrm{i}kz}\right) \\ w_1 = w_1^-(r,\theta,z) = \mathcal{R}e\left(\mathrm{i}f_w(r)e^{\mathrm{i}\theta-\mathrm{i}kz}\right) \\ q_1 = q_1^-(r,\theta,z) = \mathcal{R}e\left(f_q(r)e^{\mathrm{i}\theta-\mathrm{i}kz}\right) \end{cases} \quad (28)$$

Up to now, the boundary conditions at the ends of the cylinder, Eq. 11, have not been taken into account. In that case, the general solution at linear order of the problem consists of any linear combinations of the solutions Eqs. 15 and 28. Imposing now the boundary condition Eq. 11 yields the unique (up to the buckling amplitude) solution of the complete problem at linear order:

$$\begin{aligned} u_1 &= f_u(r)\sin\theta\sin kz \\ v_1 &= -f_v(r)\cos\theta\sin kz \\ w_1 &= -f_w(r)\sin\theta\cos kz \\ q_1 &= f_q(r)\sin\theta\sin kz \end{aligned} \quad (29)$$

with $k = n\pi/L$ and n an integer. Hence, at linear order, only discrete values of wave number k are admissible for the system to be neutral against sinusoidal perturbations, which corresponds to discrete values of the control parameter α.

In the following, we start from a value of α at which the system is neutrally stable ($\alpha = \alpha_c$), and we consider a quasi-static increase of α. The deformation is not harmonic anymore, and we calculated the expression of the corresponding mode, including the buckling amplitude.

IV. WEAKLY NON-LINEAR ANALYSIS

A. Introduction

In this section, we carry out a Koiter expansion [21–27] of the bifurcated solution in the vicinity of a bifurcation point. The displacement field and the Lagrange multiplier are expanded to order 3 in terms of an arc-length parameter ε defined as [28]:

$$\alpha = \alpha_c + \alpha_2\varepsilon^2 \quad (30)$$

$$\mathbf{t}(\alpha) = \mathbf{t}_0(\alpha) + \varepsilon\mathbf{t}_1 + \varepsilon^2\mathbf{t}_2 + \varepsilon^3\mathbf{t}_3 + \cdots \quad (31)$$

where α_c is the critical dimensionless angular velocity determined from the linear bifurcation analysis, see Eq. 23. The base solution $\mathbf{t}_0$ depends on the load α through q_0. $\mathbf{t}_1$ is the linear mode calculated in Section III and normalized so that the buckling amplitude is $\varepsilon\xi$. The Koiter method proceeds by inserting the expansion in Eqs. 30–31 into the non-linear equilibrium written earlier in Eq. 4 as

$$\forall\delta\mathbf{t}, \quad D\mathcal{E}\left(\alpha_c+\alpha_2\varepsilon^2, \mathbf{t}_0(\alpha)+\varepsilon\mathbf{t}_1+\varepsilon^2\mathbf{t}_2+\varepsilon^3\mathbf{t}_3+\cdots\right)[\delta\mathbf{t}] = 0, \quad (32)$$

where $\delta\mathbf{t}(r,\theta,z)$ is the set of virtual functions $\left(\delta u, \delta v, \delta w, \delta q\right)$ that represent infinitesimal increments of the displacements (including the Lagrange multiplier) satisfying the kinematic boundary conditions. Eq. 32 is then expanded order by order in ε [27–29]. The linear bifurcation problem is recovered at order ε :

$$\forall\delta\mathbf{t}, \quad D^2\mathcal{E}\left(\alpha_c\right)[\mathbf{t}_1, \delta\mathbf{t}] = 0. \quad (33)$$

B. Second-order correction to the displacement

Order ε^2 of Eq. 32 yields the equations for the second-order correction $\mathbf{t}_2 = (u_2, t_2, z_2, q_2)$. $\mathbf{t}_2$ results from the non-linear interaction of the linear mode $\mathbf{t}_1$ with itself. As a result, it involves a superposition of Fourier modes having wave numbers $\pm k$ with respect to the variable z, and circumferential wave numbers ± 1. Hence, we seek the second-order correction $\mathbf{t}_2$ to the displacement as:

$$\begin{aligned} u_2(r,\theta,z) =& g_{u1}(r) + g_{u2}(r)\sin(2kz) + g_{u3}(r)\cos(2kz) + g_{u4}(r)\sin(2\theta) + g_{u5}(r)\cos(2\theta) + g_{u6}\sin(2\theta)\sin(2kz) \\ &+ g_{u7}\sin(2\theta)\cos(2kz) + g_{u8}(r)\cos(2\theta)\sin(2kz) + g_{u9}(r)\cos(2\theta)\cos(2kz) \end{aligned} \tag{34}$$

$$\begin{aligned} v_2(r,\theta,z) =& g_{v1}(r) + g_{v2}(r)\sin(2kz) + g_{v3}(r)\cos(2kz) + g_{v4}(r)\cos(2\theta) + g_{v5}(r)\sin(2\theta) + g_{v6}(r)\cos(2\theta)\sin(2kz) \\ &+ g_{v7}(r)\cos(2\theta)\cos(2kz) + g_{v8}\sin(2\theta)\sin(2kz) + g_{v9}\sin(2\theta)\cos(2kz) \end{aligned} \tag{35}$$

$$\begin{aligned} w_2(r,\theta,z) =& g_{w1}(r) + g_{w2}(r)\cos(2kz) + g_{w3}(r)\sin(2kz) + g_{w4}(r)\sin(2\theta) + g_{w5}(r)\cos(2\theta) + g_{w6}\sin(2\theta)\cos(2kz) \\ &+ g_{w7}\sin(2\theta)\sin(2kz) + g_{w8}(r)\cos(2\theta)\cos(2kz) + g_{w9}(r)\cos(2\theta)\sin(2kz) \end{aligned} \tag{36}$$

$$\begin{aligned} q_2(r,\theta,z) =& g_{q1}(r) + g_{q2}(r)\sin(2kz) + g_{q3}(r)\cos(2kz) + g_{q4}(r)\sin(2\theta) + g_{q5}(r)\cos(2\theta) + g_{q6}\sin(2\theta)\sin(2kz) \\ &+ g_{q7}\sin(2\theta)\cos(2kz) + g_{q8}(r)\cos(2\theta)\sin(2kz) + g_{q9}(r)\cos(2\theta)\cos(2kz). \end{aligned} \tag{37}$$

The calculation of the deformation at order ε^2 requires to take into account a series expansion of the dimensionless strain energy W at order 2 in terms of $I_1 - 3$ and $I_2 - 3$. Here, we consider the most general form for this expansion, without any restriction to a specific kind of constitutive equation:

$$W = \frac{1}{2}\beta(I_1-3) + \frac{1}{2}(1-\beta)(I_2-3) + \gamma_{11}(I_1-3)^2 + \gamma_{12}(I_1-3)(I_2-3) + \gamma_{22}(I_2-3)^2\cdots, \tag{38}$$

where β, γ_{11}, γ_{12} and γ_{22} are constant parameters that depend on the material properties. For instance, $\beta = 1$ and $\gamma_{11} = \gamma_{12} = \gamma_{22} = 0$ for an incompressible neo-Hookean solid [11, 17], and $\gamma_{11} = \gamma_{12} = \gamma_{22} = 0$ for an incompressible Mooney-Rivlin solid [18, 19].

The expressions of the functions $g(r)$ defined in Eq. 34-37 are found by solving at order ε^2 the differential equations Eqs. 6-9 with the boundary conditions Eqs. 10. The detailed expressions of these functions are written explicitly in the Appendix, in terms of ξ, k, r_0, β and $\gamma = \gamma_{11} + \gamma_{12} + \gamma_{22}$.

C. Amplitude equation

Order ε^3 of Eq. 32 yields:

$$\begin{aligned} \forall\delta\mathbf{t}, \quad & D^2\mathcal{E}(\alpha_c, \mathbf{t}_0(\alpha_c))\cdot[\mathbf{t}_3, \delta\mathbf{t}] + D^3\mathcal{E}(\alpha_c, \mathbf{t}_0(\alpha_c))\cdot[\mathbf{t}_2, \mathbf{t}_1, \delta\mathbf{t}] \\ & + \alpha_2 \left.\frac{\mathrm{d}D^2\mathcal{E}(\alpha, \mathbf{t}_0(\alpha))}{\mathrm{d}\alpha}\right|_{\alpha=\alpha_c}\cdot[\mathbf{t}_1, \delta\mathbf{t}] + \frac{1}{6}D^4\mathcal{E}(\alpha_c, \mathbf{t}_0(\alpha_c))\cdot[\mathbf{t}_1, \mathbf{t}_1, \mathbf{t}_1, \delta\mathbf{t}] = 0. \end{aligned}$$

$D^2\mathcal{E}[\delta\mathbf{t}; \mathbf{t}_1]$ denotes the second Gâteaux derivative of $\mathcal{E}$, which is a bi-linear symmetric form on the increment $\mathbf{t}_1$ and on the virtual increment $\delta\mathbf{t}$. Similarly, $D^3\mathcal{E}[\delta\mathbf{t}; \mathbf{t}_1; \mathbf{t}_2]$ is the third Gâteaux derivative (a tri-linear symmetric form), etc. Insertion of the particular virtual displacement $\delta\mathbf{t} = \mathbf{t}_1$ enforces compatibility of the ε^2-order equilibrium equations (Fredholm solvability condition). The first term cancels out by Eq. 33 and we are left with

$$D^3\mathcal{E}(\alpha_c, \mathbf{t}_0(\alpha_c))\cdot[\mathbf{t}_2, \mathbf{t}_1, \mathbf{t}_1] + \alpha_2 \left.\frac{\mathrm{d}D^2\mathcal{E}(\alpha, \mathbf{t}_0(\alpha))}{\mathrm{d}\alpha}\right|_{\alpha=\alpha_c}\cdot[\mathbf{t}_1, \mathbf{t}_1] + \frac{1}{6}D^4\mathcal{E}(\alpha_c, \mathbf{t}_0(\alpha_c))\cdot[\mathbf{t}_1, \mathbf{t}_1, \mathbf{t}_1, \mathbf{t}_1] = 0. \tag{39}$$

The quantities appearing Eq. 39 are calculated with the help of a symbolic calculation language from the explicit expression of the functions f (linear order) and the functions g (second order):

$$D^3\mathcal{E}(\alpha_c, \mathbf{t}_0(\alpha_c))\cdot[\mathbf{t}_2, \mathbf{t}_1, \mathbf{t}_1] = \frac{\mu\pi^2 r_0^2}{k}\left(\frac{\xi}{r_0}\right)^4\left\{-\frac{3(kr_0)^4}{8}(16\gamma - 2\beta + 1) + (kr_0)^6(2\gamma - \frac{5}{16}) + \cdots\right\}, \tag{40}$$

$$D^4\mathcal{E}(\alpha_c, \mathbf{t}_0(\alpha_c))\cdot[\mathbf{t}_1, \mathbf{t}_1, \mathbf{t}_1, \mathbf{t}_1 = \frac{\mu\pi^2 r_0^2}{k}\left(\frac{\xi}{r_0}\right)^4\left\{\frac{9(kr_0)^4}{2}(8\gamma - \beta + 1) - \frac{3(kr_0)^6}{8}(32\gamma - 6\beta + 7) + \cdots\right\}, \tag{41}$$

$$\left.\frac{\mathrm{d}D^2\mathcal{E}(\alpha, \mathbf{t}_0(\alpha))}{\mathrm{d}\alpha}\right|_{\alpha=\alpha_c} = -\frac{\mu\pi^2 r_0^2}{k}\frac{1}{2}\left(\frac{\xi}{r_0}\right)^2. \tag{42}$$

Eq. 39 then yields the sought relation between the scaled load increment α_2 and amplitude ξ:

$$\alpha_2 = \kappa \frac{\xi^2}{r_0^2}, \tag{43}$$

with

$$\kappa = \frac{3}{4}(kr_0)^4 + \frac{3}{4}(\beta - 2)(kr_0)^6 + \left(\frac{27}{8}\gamma - \frac{3}{32}\beta^2 - \frac{61}{96}\beta + \frac{105}{128}\right)(kr_0)^8 + \cdots \tag{44}$$

Multiplying both sides of Eq. 43 by ε^2 and identifying (i) the load increment $\alpha - \alpha_c$ from Eq. 30 and (ii) the true buckling amplitude $\zeta = \varepsilon\,\xi$, we find the amplitude equation as

$$\left(\frac{\zeta}{r_0}\right)^2 = \frac{1}{\kappa}\left(\alpha - \alpha_c\right). \tag{45}$$

κ is plotted as a function of kr_0 for different constitutive laws in Figure 3. The order in the expansion in kr_0 in

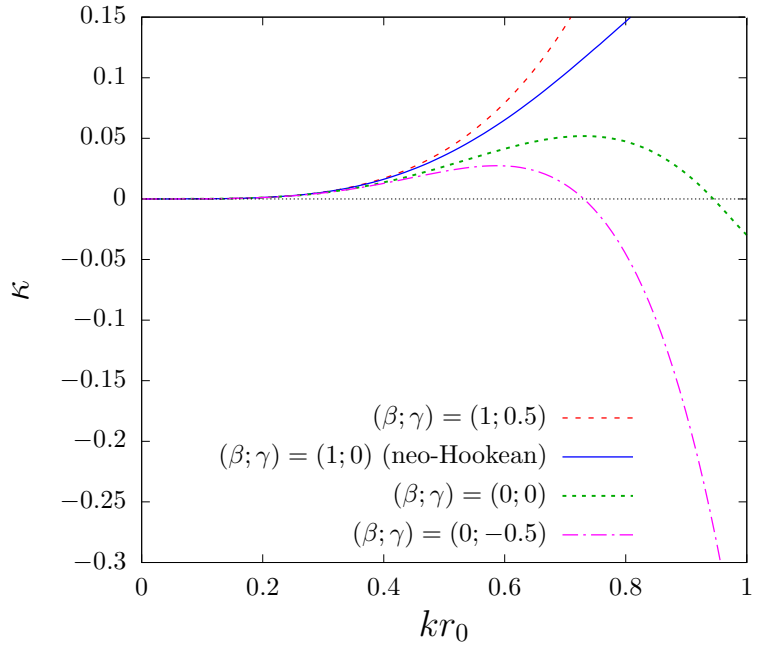

FIG. 3: κ defined by Eq. 44 calculated from series expansions at order 30 in kr_0 for a neo-Hookean constitutive law $(\beta;\gamma) = (1;0)$; two Mooney-Rivlin constitutive laws $(\beta;\gamma) = (0.5;0)$ and $(\beta;\gamma) = (1;0)$; and a constitutive law with $(\beta;\gamma) = (0;-0.5)$.

Eq. 44 is high enough to have no visible effect of it in this plot. Interestingly, κ can be positive or negative, depending on the constitutive law and on the values of kr_0. Based on the amplitude equation in Eq. 45, the bifurcation is super critical (continuous) if $\kappa > 0$ ($\zeta = r_0\sqrt{(\alpha - \alpha_c)/\kappa}$) and sub-critical (discontinuous) otherwise ($\zeta = r_0\sqrt{(\alpha_c - \alpha)/\kappa}$). The bifurcated branch is found above the critical load α_c in the super critical case, and below α_c in the sub critical case. In both cases, the base state is stable against perturbations of wave number k below the linear threshold α_c, and unstable beyond this threshold. One deduces from the Leray-Schauder rule [30] that super critical bifurcated branches are stable while sub critical branches are unstable.

V. COMPARISON WITH FINITE ELEMENT SIMULATIONS

In this section, the complete non-linear problem defined by Eq. 4 is implemented by using the open source tool for solving partial differential equations FEniCS [31]. The goal is to check whether the numerical simulations well capture the results of both the linear and the non-linear analysis of sections III-IV.

We consider a semicircular solid cylinder Ω of radius r_0 and height $2\pi/k$. A Cartesian coordinates system (x, y, z) with the base vectors $(\mathbf{e}_x, \mathbf{e}_y, \mathbf{e}_z)$ is chosen such that $(x, y, z) \in \Omega \Leftrightarrow \sqrt{x^2 + y^2} \leq r_0$, $x \geq 0$ and

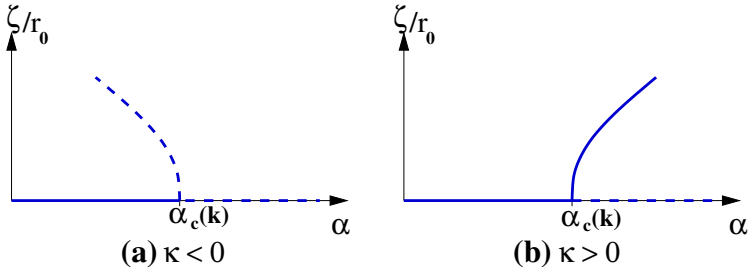

FIG. 4: Sketches of the buckling amplitude close to the bifurcation point. (a) for $\kappa < 0$ the bifurcation is sub-critical. (b) for $\kappa > 0$ the bifurcation is super-critical. Solid lines represent stable points against perturbations of wave number k, while dotted lines represent unstable one.

$0 \leq z \leq 2\pi/k$. An incompressible and isotropic elastic solid (mass density ρ ; shear modulus μ) occupying the domain Ω in its reference configuration is subjected to the action of the centrifugal volume force $\rho\omega^2(x\mathbf{e}_x + y\mathbf{e}_y)$. The lateral surface ($\sqrt{x^2+y^2} = r_0$) of the cylinder is traction free, the displacements in the direction of $\mathbf{e}_x$ are set to zero for $x = 0$ (so that $x = 0$ is a plane of symmetry), and periodic boundary conditions along axis z with wave number k are implemented by mapping the boundary of Ω in plane $z = 0$ to the boundary in plane $z = L$.

The displacement vector $\mathbf{u}$ is discretized using Lagrange finite elements with a quadratic interpolation, and the Lagrange multiplier q with a linear interpolation. The non-linear problem in $\mathbf{u} - q$ is solved using a Newton algorithm based on a direct parallel solver (`MUMPS`) [32]. Quasi-static simulations are performed by setting $\mu = 1$, $r_0 = 1$, and slowly varying $\alpha \equiv \rho\omega^2$ up to the desired value. For each α the displacement field and the Lagrange multiplier are computed. Simulations are carried out for different values of the wave number and different elastic constitutive laws.

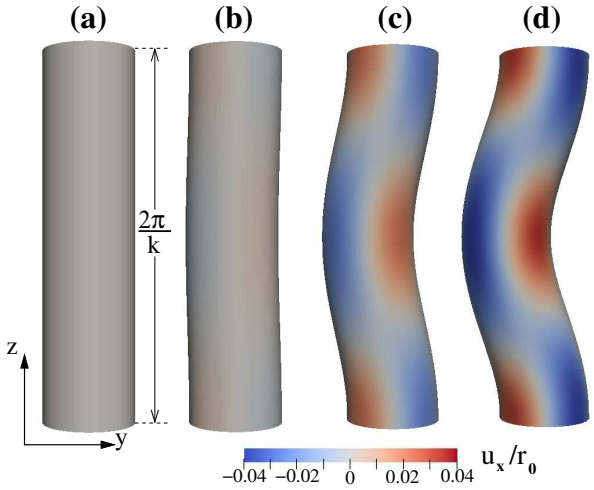

FIG. 5: Snapshots from FEM simulations of a neo-Hookean spinning cylinder with $kr_0 = \frac{\pi}{4}$, for $\frac{\alpha-\alpha_c}{\alpha_c} = 0$ (a), 8.4×10^{-4} (b), 4.2×10^{-2} (c) and 0.1 (d). The buckling amplitudes are respectively equal to 0 (a), 0.037 (b), 0.29 (c) and 0.45 (d). Colors indicate the normalized displacement along x-direction, u_x/r_0.

Starting from the undisturbed base system ($\mathbf{u} = 0$), α is gradually increased with increments $\delta\alpha = 1/100000$. The deformation is almost zero until a critical value of α for which the deformation begins to increase (as a function of α) abruptly. Due to the boundary conditions imposed in the simulations, these deformations are consistent with those investigated in Secs. III-IV (see Figure 5). Accordingly with the definition in Section IV C of buckling amplitude ζ, the buckling amplitude in the simulations is computed as the maximum displacement of the material points located at the lateral boundary of the cylinder. The normalized buckling amplitude ζ/r_0 computed from the simulations for a neo-Hookean constitutive law and the wave number $kr_0 = \pi/15$ is plotted as a function of α in Figure 6. Fitting

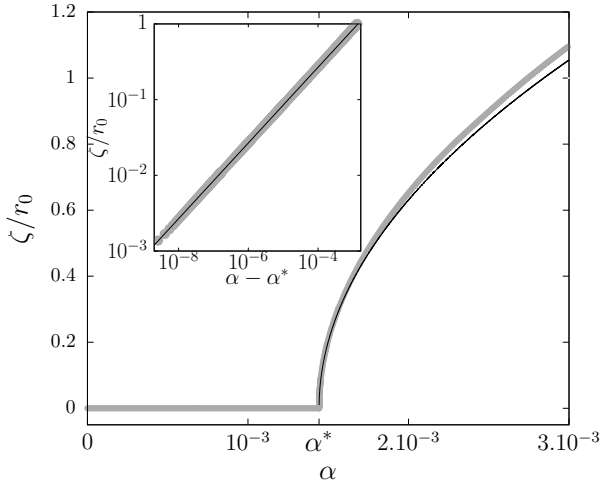

FIG. 6: Gray symbols: Normalized buckling amplitude ζ/r_0 as a function of α for the neo-Hookean constitutive law, obtained by FEM simulations for $kr_0 = \pi/15$. Solid line is obtained by fitting $\zeta/r_0 = \sqrt{(\alpha - \alpha^*)/\kappa^*}$ via α^* and κ^*: $\alpha^* = 0.00144$ and $\kappa^* = 0.00137$. Inset : same data plotted in log-scales.

ζ/r_0 with the function $f(\alpha)$ defined by :

$$\begin{aligned} f(\alpha) &= 0 \quad \text{for} \quad \alpha < \alpha^* \\ f(\alpha) &= \sqrt{(\alpha - \alpha_c)/\kappa^*} \quad \text{for} \quad \alpha > \alpha^*, \end{aligned} \tag{46}$$

for $\zeta/r_0 < 0.2$ gives values of the threshold α^* computed from the simulations, as well as the coefficient κ^*.

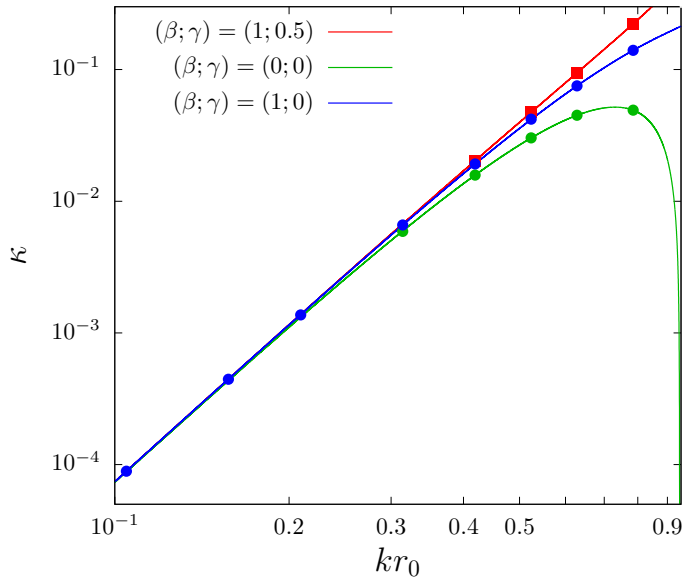

FIG. 7: κ as a function of kr_0 in log-log scale for different constitutive laws. Solid lines result from of Eq. 44 (calculated at order 30 in kr_0; the plot would not change by increasing the order). Filled circles results from fits of the buckling amplitude calculated by FEM simulation, as presented in Figure 6.

In Figure 2, α^* is plotted together with the theoretical prediction of the linear threshold, Eq. 23. A comparison of κ^* with the theoretical prediction based on the weakly non-linear analysis, Eq. 44, is shown in Figure 7 for different wave numbers and different constitutive laws. The good agreement between theory and simulations clearly validates the results of Sections III and IV. In addition, the simulations show that the prediction of Eqs. 44-45 remains good for finite values of ζ/r_0 (Figure 6). Discrepancies with the square root expression of the weakly non-linear analysis are

barely observable in log-log scales (inset of Figure 6). For instance, for a neo-Hookean constitutive law and $kr_0 = 15\pi$, differences are smaller than 1% for $\zeta/r_0 < 90\%$.
The sub-critical nature of the bifurcation, unveiled in Figure 3 for certain values of β and γ and certain values of the wave number, is also captured by the FEM simulations. In those cases, the load α has to be gradually decreased from a value larger than the instability threshold, and the buckling amplitude is found to grow as α continues to decrease below the critical load (Figure 8). For these sub-critical bifurcations, the range of the load in which the buckling amplitude follows a square root law is more reduced compared to the super-critical case.

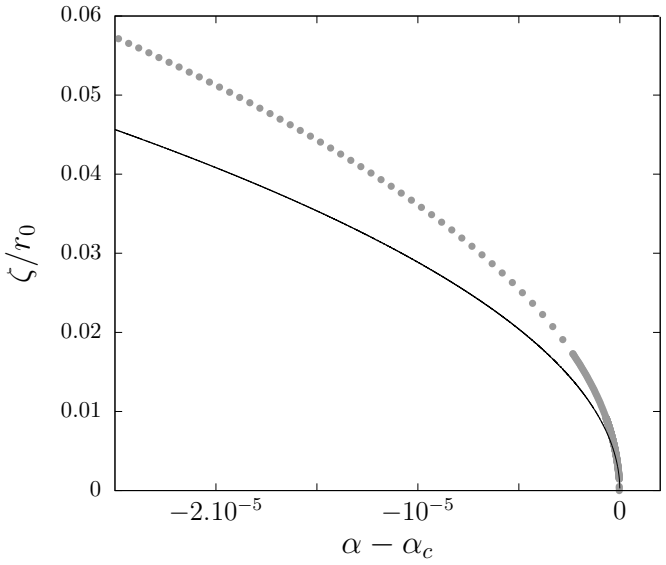

FIG. 8: Filled circles: Normalized buckling amplitude ζ/r_0 as a function of α for a Mooney-Rivlin constitutive law with $\beta = 0$, obtained by FEM simulations for $kr_0 = \pi/3.25$. Solid line is the prediction of the weakly non-linear theory of Section IV.

VI. CONCLUDING REMARKS

The stability of spinning cylinders against perturbations of given wave number has been investigated. Bifurcations occur for discrete wave numbers and are related to critical values of the control parameter α. The non-linearities driving the buckling amplitude arise both from the geometry and the elastic response of the material. They simultaneously appear at order 2 in expansions with respect to the amplitude of the deformations. The buckling amplitude has been calculated in the weakly non-linear regime for different wave numbers and for any isotropic and isochoric constitutive law of the elastic material. Since the calculation relies on a Koiter expansion of the deformation calculated from a base undeformed configuration, the obtained analytic expression is limited to infinitesimal deformations. It has been complemented with numerical simulations, showing that the analytic expression is indeed relevant beyond the limit of the small infinitesimal deformations.

Upon a gradual increase of α from zero, the wave number of the first mode that develops is $k = \pi/L$. The condition $r_0 \ll L$ implies $kr_0 \ll 1$ for this mode. Within this limit, $\alpha_c \sim \kappa \sim \frac{3}{4}(kr_0)^4$ (from Eqs. 23 and 44). Hence,

$$\zeta = r_0\sqrt{\alpha/\alpha_c - 1}. \tag{47}$$

This formula differs from the expression proposed in [9] and established in the long wave length limit through a one-dimensional model and by ignoring material non-linearities. This discrepancy shows that an approach based on Hookean elasticity for calculating the buckling amplitude is not relevant even in the long wave length limit. Indeed, calculating the buckling amplitude using reduction to one dimensional model would require a reduction consistent with the non-linear material constitutive law of the elastic material [33].

Non-linearities in the elastic material properties are a key ingredient for the study of the whirling instability: the buckling amplitude at the instability onset, and also the nature of the bifurcation (sub-critical or super-critical) depend on the coefficients appearing in the second order expansion of the strain energy density. Indeed, non-linear elastic properties are important in many systems or devices in which elastic bodies are subjected to finite deformations, as

in soft robotics and surgery. As in the whirling instability investigated here, these deformations can be associated to instabilities [34–36] that lead to dramatic change in the system behaviour. The development of rigorous frameworks and methodologies for predicting, understanding and analysing these instabilities is then an important task.

The deformations considered in this paper being stationary, the equilibrium configurations have been analyzed by minimizing the total energy of the system, since energy dissipation processes are not relevant. A study of the issue of the transient regimes, *i.e.* the way the previously investigated steady states are reached, would required more complex formulations in which the dissipative processes have to be accounted for together with the material and geometric non-linearities in dynamical equations.

Acknowledgments: Corrado Maurini is thanked for his help with FEniCS.

Conflict of Interest: The author declares that he has no conflict of interest.

[1] E. Krämer, editor. *Dynamics of Rotors and Foundations*. Springer-Verlag, 1993.
[2] G. Genta, editor. *Dynamics of Rotating Systems*. Springer, 2005.
[3] W.J. Chen and E.J. Gunter, editors. *Introduction to Dynamics of Rotor-Bearing Systems*. Trafford, 2005.
[4] F.F. Ehrich. Shaft whirl induced by rotor internal damping. *Journal of Applied Mechanics*, 31:279–282, 1964.
[5] S. Noah and P. Sundarajan. Significance of considering nonlinear effects in predicting the dynamic behavior of rotating machinery. *J. Vib. Control*, 1:431–458, 1995.
[6] T. Yamamoto and Y. Ishida, editors. *Linear and Nonlinear Rotordynamics: A Modern Treatment with Applications*. Wiley, 2012.
[7] J. Shaw and S.W. Shaw. Instabilities and bifurcations in a rotating shaft. *Journal of Sound and Vibration*, 132:227–244, 1989.
[8] W. Kurnik. Stability and bifurcation analysis of a nonlinear transversally loaded rotating shaft. *Nonlinear Dyn.*, 5:39–52, 1994.
[9] S.A.A. Hosseini. Dynamic stability and bifurcation of a nonlinear in-extensional rotating shaft with internal damping. *Nonlinear Dyn.*, 74:345–358, 2013.
[10] D. Henry, editor. *Geometric Theory of Semi-Linear Parabolic Equations*. Springer, 1981.
[11] R.W. Ogden. *Non-Linear Elastic Deformations*. Ellis Horwood Limited, Chichester, 1984.
[12] H.W Haslach. Post-buckling behavior of columns with non-linear constitutive equations. *Int. J Non-Linear Mechanics*, 20:53–267, 1985.
[13] L. Cveticanin. Large in-plane motion of a rotor. *Journal of Vibration and Acoustics*, 120:267–282, 1998.
[14] D.M. Haughton and R.W. Ogden. Bifurcation of finitely deformed rotating elastic cylinders. *Q. J. Mech. appl. Math.*, 33:251–265, 1980.
[15] F. Richard, A. Chakrabarti, B. Audoly, Y. Pomeau, and S. Mora. Buckling of a spinning elastic cylinder: linear, weakly nonlinear and post-buckling analyses. *Proc. R. Soc. A*, 474:20180242, 2018.
[16] S. Mora and F. Richard. Buckling of a compliant hollow cylinder attached to a rigid shaft. *International Journal of Solids and Structures*, 167:142–155, 2019.
[17] C.W. Macosko. *Rheology : principles , measurements and applications*. Wiley-VCH, New York, 1994.
[18] M. Mooney. A theory of large elastic deformation. *Journal of Applied Physics*, 11:582–592, 1940.
[19] R.S. Rivlin. Large elastic deformations of isotropic materials. iv. further developments of the general theory. *Philosophical Transactions of the Royal Society of London. Series A, Mathematical and Physical Sciences*, 241:379–397, 1948.
[20] R. Gâteaux. Fonctions d'une infinité de variables indépendantes. *Bulletin de la Société Mathématique de France*, 47:70–96, 1919.
[21] W. T. Koiter. *On the stability of an elastic equilibrium*. PhD thesis, Techische Hooge School Delft, 1945.
[22] J. W. Hutchinson. Imperfection sensitivity of externally pressurized spherical shells. *Journal of Applied Mechanics*, 34:49–55, 1967.
[23] J. W. Hutchinson and W.T. Koiter. Postbuckling theory. *Applied Mechanics Reviews*, pages 1353–1366, 1970.
[24] B. Budiansky. Theory of buckling and post-buckling behavior of elastic structures. *Advances in applied mechanics*, 14:1–65, 1974.
[25] R. Peek and N. Triantafyllidis. Worst shapes of imperfections for space trusses with many simultaneously buckling members. *International Journal of Solids and Structures*, 29:2385–2402, 1992.
[26] R. Peek and M. Kheyrkhahan. Postbuckling behavior and imperfection sensitivity of elastic structures by the Lyapunov-Schmidt-Koiter approach. *Computer methods in applied mechanics and engineering*, 108(3):261–279, 1993.
[27] A. van der Heijden. *W. T. Koiter's elastic stability of solids and structures*. Cambridge University Press Cambridge, 2009.
[28] A. Chakrabarti, S. Mora, F. Richard, T. Phou, J.M. Fromental, Y. Pomeau, and B. Audoly. Selection of hexagonal buckling patterns by the elastic rayleigh-taylor instability. *Journal of the Mechanics and Physics of Solids*, 121:234–257, 2018.

[29] Nicolas Triantafyllidis. *Stability of solids: From Structures to materials*. Ecole Polytechnique, 2011.
[30] C. Normand, Y. Pomeau, and M. G. Velarde. Convective instability: a physicist's approach. *Reviews of Modern Physics*, 49(3):581, 1977.
[31] A. Logg, K.A. Mardal, and G. Wells. *Automated Solution of Differential Equations by the Finite Element Method*. Springer, 2012.
[32] PR Amestoy, IS Duff, JY L'Escellent, and J. Koster. A fully asynchronous multifrontal solver using distributed dynamic scheduling. *SIAM Journal on Matrix Analysis and Applications*, 23:15–41, 2001.
[33] C. Lestringant and B. Audoly. Asymptotically exact strain-gradient models for nonlinear slender elastic structures: A systematic derivation method. *Journal of the Mechanics and Physics of Solids*, page 103730, 2019.
[34] S. Mora, M. Abkarian, H. Tabuteau, and Y. Pomeau. Surface instability of soft solids under strain. *Soft Matter*, 7:10612–10619, 2011.
[35] S. Mora, T. Phou, J. M. Fromental, and Y. Pomeau. Gravity driven instability in solid elastic layers. *Phys. Rev. Lett.*, 113:178301, 2014.
[36] S. Mora, E. Ando, T. Phou, J. M. Fromental, and Y. Pomeau. The shape of hanging elastic cylinders. *Soft Matter*, 15:5464, 2019.

Appendix A: Expression of the functions defining the second order correction to the displacement

The expressions of the functions g defined by Eqs. 34-37 are given in this appendix. These expressions are obtained by inserting Eqs. 30-31 into Eqs. 6-9 and in the boundary conditions Eqs. 10 at order ε^2.

$$
\begin{aligned}
g_{u1}(r) &= \frac{\xi^2}{r_0}\left\{-\frac{r}{4r_0}(r_0k)^2+\left(4\frac{r}{r}-\frac{r^3}{r_0^3}\right)\frac{(kr_0)^4}{32}+\left(7\frac{r}{r_0}-6\frac{r^3}{r_0^3}+2\frac{r^5}{r_0^5}\right)\frac{(kr_0)^6}{128}+\cdots\right\}\\
g_{u3}(r) &= \frac{\xi^2}{r_0}\left\{-\frac{r}{8r_0}(kr_0)^2-\left((2\beta-9)\frac{r}{r_0}+3\frac{r^3}{r_0^3}\right)\frac{(kr_0)^4}{32}+\left((116\beta-230)\frac{r}{r_0}+54\frac{r^3}{r_0^3}+(12\beta-33)\frac{r^5}{r_0^5}\right)\frac{(kr_0)^6}{1152}+\cdots\right\}\\
g_{u5}(r) &= \frac{\xi^2}{r_0}\left\{\frac{r}{8r_0}(kr_0)^2-\frac{r^3}{16r_0^3}(kr_0)^4+\left((150\beta-269)\frac{r}{r_0}+(20\beta+198)\frac{r^3}{r_0^3}+(-30\beta-19)\frac{r^5}{r_0^5}\right)\frac{(kr_0)^6}{1536}+\cdots\right\}\\
g_{u9}(r) &= \frac{\xi^2}{r_0}\left\{\frac{r}{8r_0}(kr_0)^2-\left(6\frac{r}{r_0}-3\frac{r^3}{r_0^3}\right)\frac{(kr_0)^4}{16}+\left((2\beta+561)\frac{r}{r_0}+(60\beta-422)\frac{r^3}{r_0^3}+(-26\beta+111)\frac{r^5}{r_0^5}\right)\frac{(kr_0)^6}{1536}+\cdots\right\}
\end{aligned}
$$

$$
\begin{aligned}
g_{v5}(r) &= \frac{\xi^2}{r_0}\left\{-(\frac{r}{8r_0}(kr_0)^2-\left((150\beta-269)\frac{r}{r_0}+(40\beta-36)\frac{r^3}{r_0^3}+(-90\beta+75)\frac{r^5}{r_0^5}\right)\frac{(kr_0)^6}{1536}+\cdots\right\}\\
g_{v9}(r) &= \frac{\xi^2}{r_0}\left\{-\frac{r}{8r_0}(kr_0)^2+\left(3\frac{r}{r_0}-\frac{r^3}{r_0^3}\right)\frac{(kr_0)^4}{8}-\left((2\beta+561)\frac{r}{r_0}+(-8\beta-348)\frac{r^3}{r_0^3}+(-14\beta+49)\frac{r^5}{r_0^5}\right)\frac{(kr_0)^6}{1536}+\cdots\right\}
\end{aligned}
$$

$$
\begin{aligned}
g_{w3}(r) &= \frac{\xi^2}{r_0}\left\{-\frac{kr_0}{8}+(2\beta-5)\frac{(kr_0)^3}{32}-\left((116\beta-293)+(36\beta-63)\frac{r^4}{r_0^4}\right)\frac{(kr_0)^5}{1152}+\cdots\right\}\\
g_{w9}(r) &= \frac{\xi^2}{r_0}\left\{-\frac{r^2}{8r_0^2}(kr_0)^3-\left((16\beta-44)\frac{r^2}{r_0^2}+(-8\beta+31)\frac{r^4}{r_0^4}\right)\frac{(kr_0)^5}{192}+\cdots\right\}
\end{aligned}
$$

$$
\begin{aligned}
g_{q1}(r) &= \xi^2k^2\left\{\frac{1}{4}-\left(3-8(\beta-1-6\gamma)\frac{r^2}{r_0^2}\right)\frac{(kr_0)^2}{16}\right.\\
&\quad\left.-\left((-12\beta+29+256\gamma)+(64\beta-120-832\gamma)\frac{r^2}{r_0^2}+(-12\beta+33+320\gamma)\frac{r^4}{r_0^4}\right)\frac{(kr_0)^4}{128}+\cdots\right\}\\
g_{q3}(r) &= \xi^2k^2\left\{\left(\beta+1+4(6\gamma-\beta+1)\frac{r^2}{r_0^2}\right)\frac{(kr_0)^2}{8}\right.\\
&\quad\left.-\left((-44\beta+515+2304\gamma)+(-720\beta+252+2880\gamma)\frac{r^2}{r_0^2}+(180\beta-153-576\gamma)\frac{r^4}{r_0^4}\right)\frac{(kr_0)^4}{1152}+\cdots\right\}\\
g_{q5}(r) &= \xi^2k^2\left\{(24\gamma-4\beta+7)\frac{r^2}{r_0^2}\frac{(kr_0)^2}{8}-\left((-258\beta+489+2496\gamma)\frac{r^2}{r_0^2}+(-24\beta-74-960\gamma)\frac{r^4}{r_0^4}\right)\frac{(kr_0)^4}{384}+\cdots\right\}\\
g_{q9}(r) &= \xi^2k^2\left\{-(24\gamma-4\beta+7)\frac{r^2}{r_0^2}\frac{(kr_0)^2}{8}+\left((-218\beta+289+960\gamma)\frac{r^2}{r_0^2}+(72\beta-106-192\gamma)\frac{r^4}{r_0^4}\right)\frac{(kr_0)^4}{384}+\cdots\right\}
\end{aligned}
$$

with $\gamma = \gamma_{11} + \gamma_{12} + \gamma_{22}$. The other functions g defined in Eqs. 34-37 are equal to zero. Note that the boundary conditions Eqs. 11 at $z = 0$ and $z = L$ are fulfilled at order ε^2.